HIGH FREQUENCY LIMITATION OF GaAs TRANSIT-TIME DIODES

Y-7

Nelson Lee and Dee-Son Pan
Electrical Engineering Department
University of California, Los Angeles CA. 90024

Abstract

The high-frequency capabilities of GaAs transit-time diodes have been investigated by extensive computer simulations. The spacial effect of interband tunneling and impact ionization were included. We have found GaAs diodes can operate with significant efficiency, approximately 5% in the millimeter and sub-millimeter frequency range. These results are in agreement with a recent report of a 338 GHz GaAs TUNNETT [1].

Introduction

It has been found that GaAs diodes can operate with significant efficiency at millimeter and sub-millimeter frequencies. It was speculated GaAs IMPATTs were limited to operate at frequencies below 50 GHz, due to the long intrinsic response time of the electron. However, the inclusion of interband tunneling current in these devices can increase their frequency range into the millimeter wave regime [2,3]. The devices were named MITATTs and TUNNETTs. The theoretical investigations by Elta and Haddad [2,3] have made important contributions to the details of these devices. It was reported cutoff of the MITATTs and TUNNETTs was approximately 200 GHz. We have investigated the high frequency capabilities of GaAs diodes by including the spatially dependent interband tunneling and impact ionization in our computer simulations. We have found the devices can operate with efficiencies of 5% at 500 GHz.

Device Simulation

The GaAs diodes were simulated using a full-scale simulation program. This was accomplished by dividing the device into small space intervals and solving the basic equations governing the device operation-Poisson's eq. and the continuity eqs.-in each interval. Both impact ionization and interband tunneling were incorporated as generation mechanisms in the continuity equations. The structure of the devices simulated were p^+nn^+. The electric field in the devices were above $1x10^5$ (V/cm) for virtually the entire depleted region. As a result, there were no distinct generation or drift regions. This made the incorporation of distributed impact ionization and tunneling generation essential. The ionization coefficients used were measured by Hall and Leck [4]. The tunneling current was computed using an expression formulated by Kane [5]. The validity of Kane's formula was supported by our psuedopotential calculations of the interband tunneling matrix elements. A saturated drift velocity of $5x10^6$ (cm/sec) was used for both the electrons and holes.

An important parameter in the simulation was the width of the dead space region for impact ionization and tunneling. The carriers require a certain drift distance once they are generated before they can generate additional free carriers. Carriers generate by impact ionization or by tunneling require different dead space width. From Kane's theory [5], we found, in contrast to Ref. 2 and 3, it is more appropriate not to include tunneling dead space. Treatment of impact ionization dead space was more complex. In our simulations, we experimented with including and not included the ionization dead space. By examining the carrier generation profile for each simulation, we were able to choose the appropriate dead space for each individual case. In the simulations at the frequencies above 300 GHz, tunneling generation was found to be the dominant generation mechanism. In these cases, we used a dead space assuming the free carriers which are generating additional free carriers by impact ionization were originally generated by tunneling. For frequencies below 300 GHz, we found most free carriers were generated by ionization. In these cases, we used a shorter dead space or none at all.

Results and Discussion

In Fig. 1, the generation rate profile of impact ionization for the electrons and holes and of tunneling are plotted for the 90^o phase angle. This is for a 300 GHz p^+nn^+ diode. As shown, the tunneling generation, which is maximum at 90^o, is much weaker than impact ionization generation. For this case, a dead space for ionization due to electrons was included in the region close to the p^+n junction and no hole ionization dead space was included. A large amount of generation occurs far away from the p^+n junction. This is due to the high electric field throughout the device and the saturation of the impact ionization at the high field. Fig. 2 shows the generation profiles for a 500 GHz diode. Tunneling generation dominates for this case. A larger electron dead space was used since an electron must first tunnel and then drift until it gains enough energy to impact ionize. Again, the hole dead space was not included. Fig. 3 and Fig. 4 shows the electron profiles at phase angles 90^o, 180^o, 270^o, and 360^o for the 300 and 500 GHz diodes. No electron packet is formed in the 300 GHz diode. This is due to the saturation of the ionization in the high fields which causes impact ionization to occur throughout the device. A packet is formed, however, in the 500 GHz diode. This electron pulse travels across the device towards the nn^+ junction. In this case, the tunneling generation dominates and is localized near the p^+n junction.

Based on the profiles obtained in Figs. 3 and 4, we have estimated the effect of diffusion which was neglected in the simulation. Diffusion should have a small effect on the 300 GHz case since the slope of the carrier profile is relatively constant. Diffusion should; however, cause the electron packet in the 500 GHz diode to spread. This spreading would alter the carrier profile but should not have a large effect on the induced current waveform which is based on the total number of charge drifting through the device. Thus, the efficiency would not change much. The diffusion constant in high fields was obtained from recent Monte Carlo calculations by Shichijo and Hess [6]. The computed value, 20 cm^2/sec, was in agreement with the value used by Elta and Haddad [2,3].

Simulations were carried out for devices up to 800 GHz. Each device was designed to have the optimum transit angle for that frequency and to operate in the punch-through mode. The diodes were simulated to have a bias current density of 5000 A/sec-cm^2.

 0149-645X/82/0000-0513 $00.75

The efficiencies are plotted in Fig. 5. Our findings are consistent with the 338 GHz abrupt junction TUNNETT reported by Nishizawa et al [1]. Their diode was doped at 10^{18} cm^{-3} which according to our findings, is too high to obtain a good efficiency at 338 GHz. We expect such a device would operate with higher efficiency for frequencies between 400 and 500 GHz. An abrupt junction GaAs diode should be capable of operating at 500 GHz with an efficiency of 5%.

Acknowledgements

One of the authors (D.S. Pan) would like to thank Professor G. Haddad and Professor C. Dalman for their discussions and encouragements. This work was supported by NSF contract no. ECS 81-05082.

References

1. J. Nishizawa, K. Motoya and Y. Okuno, "Proceedings of the 9th European Microwave Conference," Brighton, England, 17-20, Sept. 1979, pp 463-467, 1979.
2. M. Elta and G.I. Haddad, "Large-Signal Performance of Microwave Transit-Time Devices in Mixed Tunneling and Avalanche Breakdown". IEEE Transactions Electron Devices, Vol. ED-26, pp 941-948, June 1979.
3. M. Elta and G.I. Haddad, "High Frequency Limitations of IMPATT, MITATT, and TUNNETT Mode Devices," IEEE Trans. MTT, Vol. MTT-27, pp 442-449, May 1979.
4. G.E. Stillman, Inst. Phys. Conf. Ser. No. 33a, Chap. 4, pp 185-209, 1977.
5. E. Kane, "Zener Tunneling in Semiconductors," J. Phys. Chem. Solids, Vol. 12, pp 181-188, 1959.
6. H. Shichijo and K. Hess, "Band-Structure-Dependent Transport and Impact Ionization in GaAs," Phys. Rev. B, Vol. 23, pp 4197, April 1981.

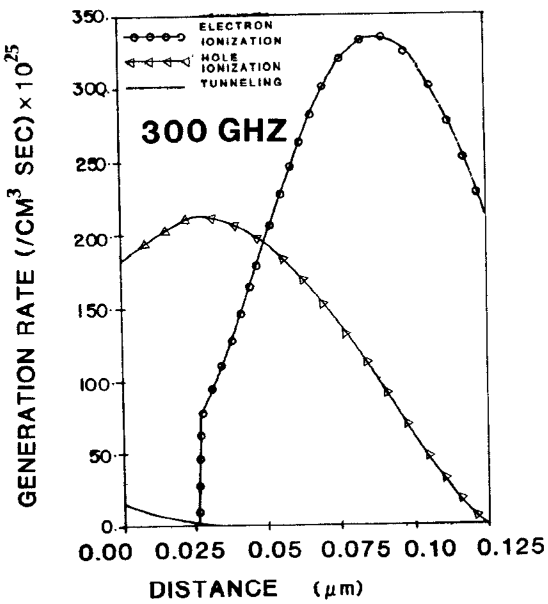

Fig. 1. Generation Profiles for: Tunneling, Impact Ionization due to Electrons and Holes at 90° Phase Angle. 300 GHz diode biased at 5000 A/cm^2.

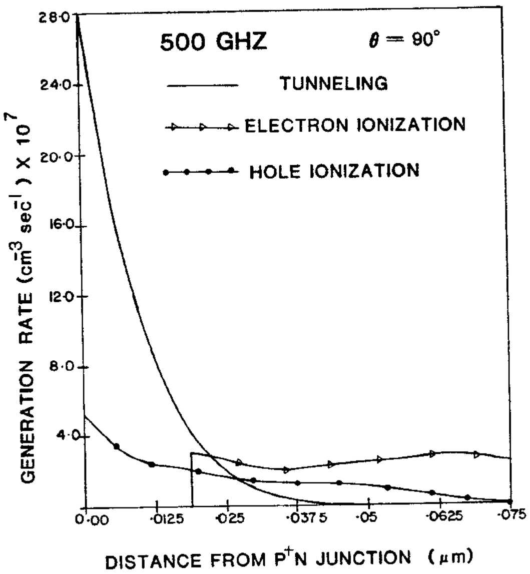

Fig. 2. Generation Profiles for: Tunneling, Impact Ionization due to Electrons and Holes at 90° Phase Angle. 500 GHz biased at 5000 A/cm^2.

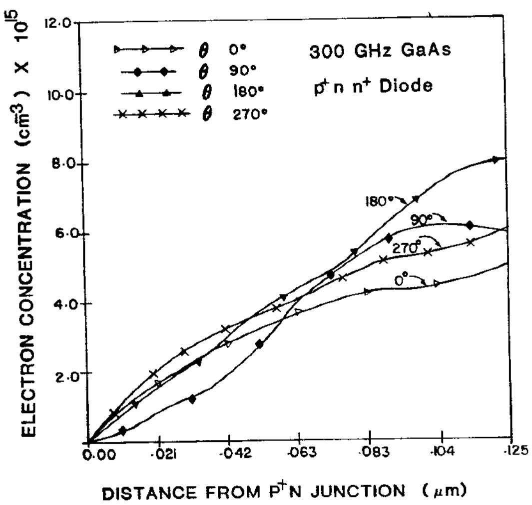

Fig. 3. Electron Carrier Profile at Various Phase Angeles. 300 GHz Diode biased at 5000 A/cm^2.

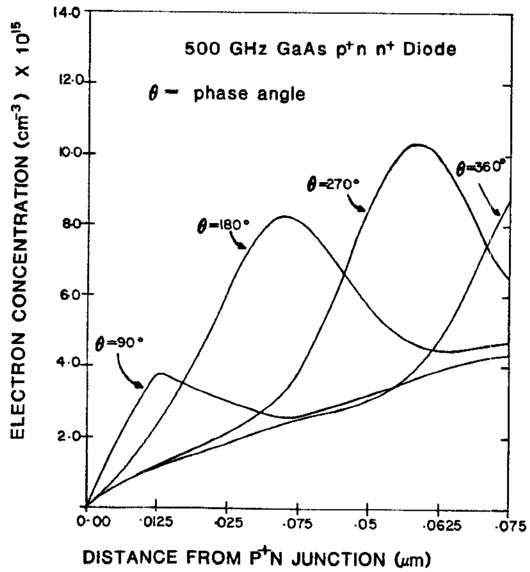

Fig. 4. Electron Carrier Profile at Various Phase Angeles. 500 GHz Diode biased at 5000 A/cm^2.

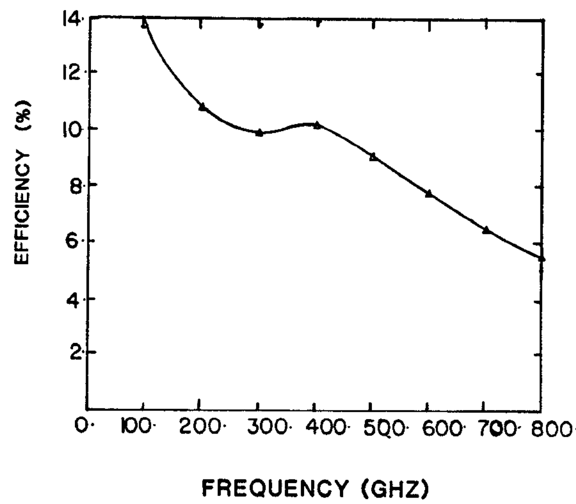

Fig. 5. Efficiency vs Frequency. Diodes biased at 5000 A/cm^2.